

Low-Cost Extracellular Voltage Amplifier for Neural Signal Acquisition

A Design Project Report

**Presented to the School of Electrical and Computer Engineering of Cornell University
in Partial Fulfillment of the Requirements for the Degree of
Master of Engineering, Electrical and Computer Engineering**

Submitted By: Gilbert Liang

M. Eng Field Advisor: Van Hunter Adams, Bruce R. Land

Outside Field Advisor: Bruce Johnson

Degree Date: May 2025

Abstract

**Master of Engineering Program
School of Electrical and Computer Engineering
Cornell University
Design Project Report**

Project Title: Low-Cost Extracellular Voltage Amplifier for Neural Signal Acquisition

Author: Gilbert Liang

Abstract: This project presents the design and validation of a low-cost extracellular voltage amplifier optimized for recording neural action potentials in educational lab environments. The amplifier features a high input impedance front-end to prevent signal loading when interfacing with various electrode types and employs a differential signal path using a precision instrumentation amplifier to achieve high common-mode rejection. Signal amplification is further performed using low-noise operational amplifiers configured in a band-pass topology with 1.5Hz to 5 kHz cutoff frequencies. These filters were implemented using inexpensive, off-the-shelf passive components. The entire system is powered by a single 9V battery, enabling portable operation while providing a stable supply rail. When tested in a classroom neurophysiology experiment using a saline suction electrode setup, the amplifier reliably captured extracellular action potential signals from motor axons of a crawfish tail and demonstrated performance comparable to commercial systems, all within a device cost of under \$50.

Executive Summary

This M.Eng project focused on developing a low-cost, portable device for recording neural signals in educational and research settings. Neural activity, such as action potentials, provides important information for understanding how the nervous system functions, but the equipment, specifically extracellular voltage amplifiers, used to measure these signals is often too expensive for use in teaching labs or resource-limited environments.

The goal of this project was to design a low-cost extracellular voltage amplifier that could be built using affordable, off-the-shelf components while providing functionality comparable to commercial systems. The final design operates on a standard 9V battery, captures low-amplitude neural signals such as action potentials, and includes basic filtering to isolate the relevant frequency range. When tested in a classroom neurophysiology lab using a saline suction electrode setup, the amplifier successfully recorded action potentials and demonstrated performance on par with a commercial amplifier used in the same environment. With a total bill-of-materials under \$50, the project offers a practical and accessible solution for neuroscience education and experimentation.

The design also allows room for future improvements, including adjustable filtering, multi-channel input, and the integration of onboard data acquisition with wireless transmission. These enhancements could further reduce system costs and eliminate the need for external lab equipment, expanding the device's usability in resource-constrained settings.

Acknowledgements

I would like to express my sincere gratitude to Professor Van Hunter Adams and Professor Bruce R. Land for their ongoing support, guidance, and encouragement throughout the course of this project. I also thank former M.Eng student Pawan Perera for his initial proof-of-concept design, providing a basis for the overall design. Additionally, I would like to acknowledge Professor Bruce R. Johnson and the BioNB/BME/ECE 4910 Student Neurophysiology Lab for providing the laboratory setup, equipment, and experimental procedures used to validate the amplifier design through the “Crawdad” lab experiment.

Introduction

In neurobiology, understanding the structure and function of the neuron, particularly its cell membrane, is essential in understanding how the nervous system operates. The cell membrane, a thin yet highly effective electrical insulator approximately 7.5 nm thick, separates the internal environment of the cell from the external space. Embedded within this membrane are protein channels that allow ions to pass in and out, establishing a resting membrane potential between -80 mV and -60 mV [1]. When sufficient ion flow occurs, a rapid electrical event known as an action potential is generated, causing a brief but significant voltage changes across the membrane. This signal change propagates along thin fibers, known as axons, enabling communication between neurons and target tissues such as muscle fibers. In motor neurons, successive action potentials initiate and sustain muscle contraction. Monitoring the timing of these signals provides valuable information, as delays may indicate damage to nerves or muscle fibers.

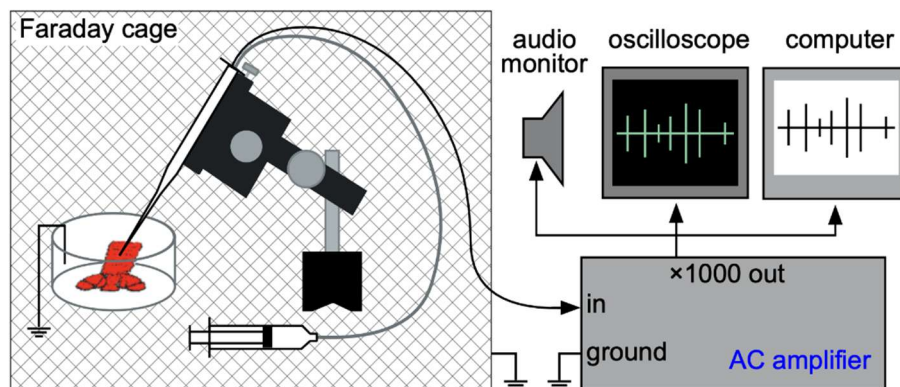


Figure 1) Extracellular Voltage Amplifier used in Lab Experiment

Extracellular measurements of neural signals typically observe voltage amplitudes ranging from 10 to 100 μ V, varying due to type of axon recorded. Given that neurons are only a few micrometers in diameter, accurate recording at this scale requires precise instrumentation. While intracellular microelectrodes can directly access the membrane, extracellular electrodes that are placed in proximity and immersed in a saline solution can provide a less invasive alternative. [2] These electrodes capture the ionic return currents in the surrounding fluid, though the signal is often attenuated by tissue layers that act as resistive voltage dividers. [1] To analyze these weak signals, this requires the signal to be amplified. However, amplification also boosts environmental and biological noise. To address this, differential electrode configurations can be used, feeding signals into a differential amplifier that suppresses common-mode noise. This

technique improves signal quality, enabling reliable detection of action potentials for experimental and diagnostic applications. Additional filtering stages are also necessary to reject unwanted frequency components and interference.

This project introduces a design that is low-cost, comparable in functionality with commercial devices, and can be built from components off-the-shelf. With this accessible device, researchers and students can study the behavior of neurophysiology through hands-on experiments in laboratories without being limited by budget constraints.

Designing Voltage Amplification and Filter Circuit

The A-M 1700 Differential AC amplifier was chosen as the optimal commercial device to compare in terms of required functionality aspects as the device was commonly used in the ECE-4910 course lab experiments. Along with selectable gain values, the amplifier has adjustable frequency cutoff ranges which allow recording of various types of neural signals that exist within certain frequency ranges and attenuating non-relevant signals. To properly record and measure signals recorded from extracellular electrodes, this would require a voltage amplification circuit that can suppress common-mode signals and out-of-band frequencies that are not relevant to the targeted recordings [1]. With the expected action potential amplitudes ranging from -20 to 100 μ V from the stimulated motor nerve of a crawfish tail, this would require voltage gain amplification of 1000, to measure a -20mV to 100mV peak to peak voltage amplitude and signals that are properly detected. [3] Additionally, with the device's high input impedance this allows various electrodes to be connected to the amplifier without effectively loading the signal and attenuating the recorded signal. [2] Lastly, the A-M 1700 has a sufficiently high CMRR of 70dB at 60Hz which is needed to suppress noise recorded from the AC-power line. [2,4] The design and specification of this device would be based on these features of the A-M 1700, with additional consideration into the device's overall power consumption and area.

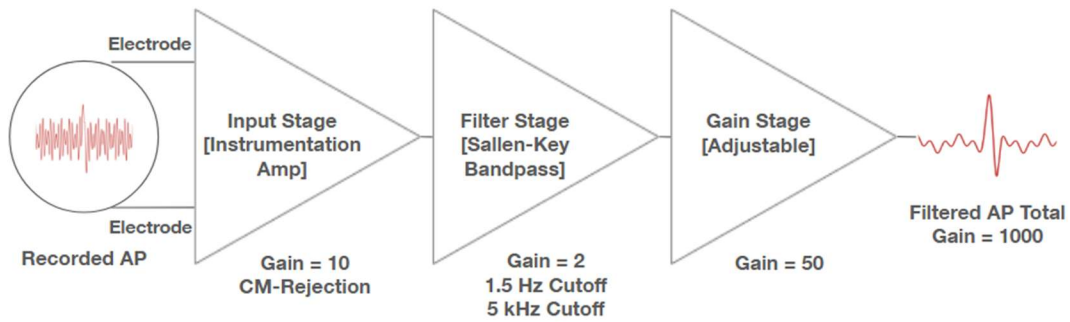


Figure 2) Block Diagram of 3-Stage Extracellular Voltage Amplifier Implementation

As this project was passed on by the previous student, Pawan Perrea, for his initial tested and validated design, the first task was to understand the overall circuit design and test through a breadboard circuit. The initial circuit design implemented a 3-stage amplification device, consisting of an instrumentation amplifier (differential input) stage, band-pass filter stage implemented through a “Sallen-Key” filter and lastly an adjustable gain stage set by a non-inverting op-amp circuit. [2,5] The circuit schematic is attached provided from Pawan’s report for the initial design that had been originally validated.

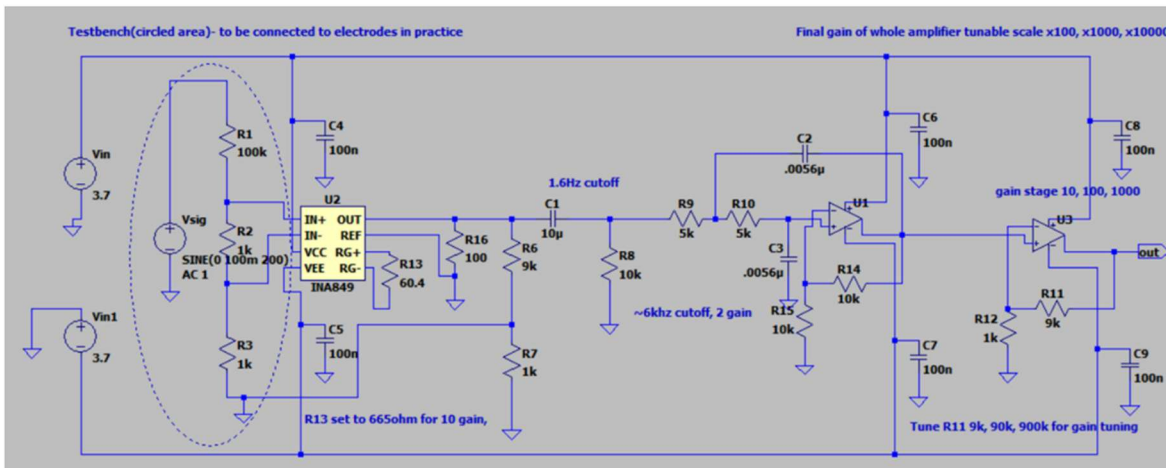


Figure 3) Pawan’s Circuit for Low-cost Extracellular Voltage Amplifier [5]

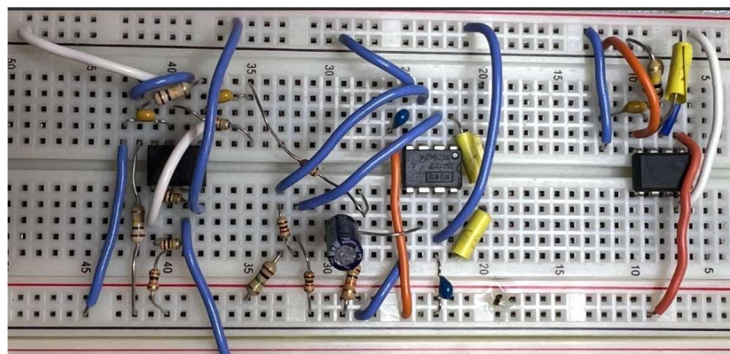


Figure 4) Breadboard circuit for Low-cost Extracellular Voltage Amplifier

The breadboard circuit was built (see Figure 4) and tested with a function generator that provided a 1V peak to peak input signal at a frequency that falls within the operating frequency range. In the initial testing of the circuit, 200Hz was chosen as this was initially done in the previous circuit for validation. [5] However, in the test replication circuit, to properly attenuate the signal and apply a gain of 1000 such that the output signal would emulate the input signal, verifying the performance and functionality, the top resistor was replaced with a 1Mega-Ohm resistor. Through the voltage divider set by R3, R4 and R5, a 1mV differential signal is applied to the input of the voltage amplifier and the input for the instrumentation stage.

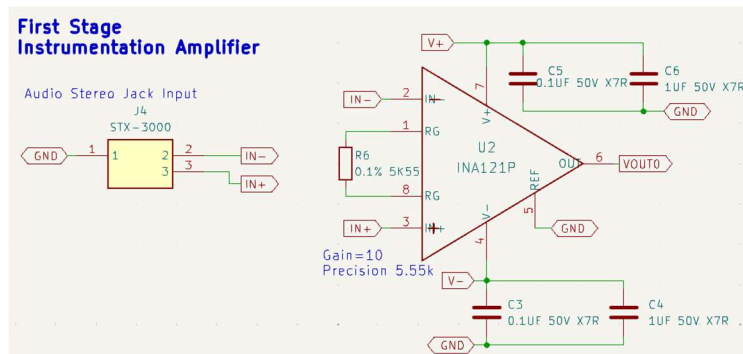


Figure 5) First Stage Instrumentation Amplifier (Rev_01)

Several components were modified after testing the initial circuit on a breadboard; The INA849 was replaced with the INA121P as this device has a much lower quiescent current, 450uA versus 2.5mA quiescent current from the INA849 which allows for an overall longer operation when powered by a 9V battery. Additionally, the INA121P has an input impedance of 1T-Ohms which meets the high-input impedance requirement that allows various electrodes to be used for the recording experiments. With a common-mode rejection of 80dB for a gain set to 10 at the highest frequency of operation (5kHz), the device is believed to be the most ideal for the project. To set the gain of this IC, a precision resistor value was calculated based on the following gain equation, provided through the technical specifications [6]:

$$G = 1 + \frac{50k\Omega}{R_G}$$

A 5.55k-Ohm resistor with extremely low tolerance (high precision) was chosen based on what was available off-the-shelf at the time, however this can be replaced with any resistor with similar value and with low tolerance. Two decouple capacitors were included, 0.1uF and 1uF on the V+ and V- supply rails, which were chosen to decouple both middle and high frequency

transient signals and stabilize the supply rail due to rippling effects that could occur from the current draw of the 3 devices in operation. As for the audio stereo jack input, this was a request made by the laboratory that would eventually use the device for testing; With a 3-pole stereo jack, this allows two differential signals to be recorded when connected to the two electrodes.

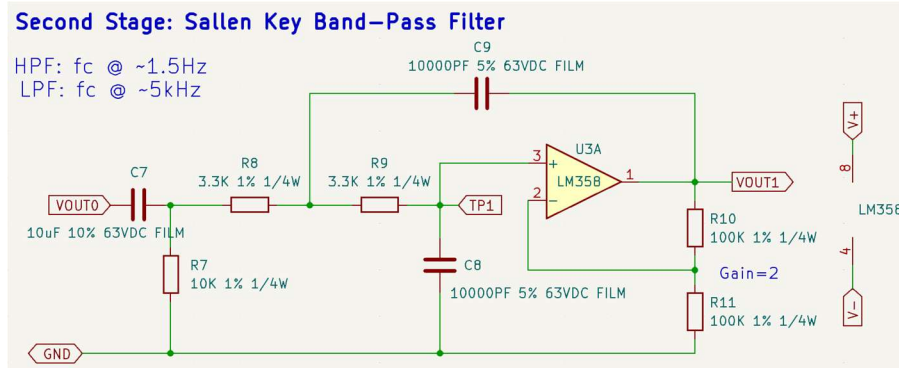


Figure 6) Second Stage Band-Pass Filter Stage (Rev_01)

To filter out the signals at frequencies outside of the operation bandwidth, a Sallen-Key bandpass circuit was implemented. The LM358 op-amp device was kept from the previous iteration as the device provided 2-op-amp channels per package, with a low quiescent current for each channel and a high unity-gain-bandwidth. For each channel of the LM358, the specified quiescent current was 300uA and a UGBW of 1.2MHz. [7] For a closed-loop gain of 2, the bandwidth for the op-amp was more than sufficient for the bandpass frequencies needed (600kHz with a gain of 2). The circuit takes the output of the first stage, that amplifies the differential signal by factor of 10 into a high-pass filter circuit of C7 and R7. The following equation determines the -3dB low cutoff frequency, where the desired cutoff frequency for the high-pass filter was defined at around 1.5Hz:

$$f = \frac{1}{2\pi\sqrt{C_7 R_7}}$$

As for setting the low-pass filter (high frequency cut-off) and to achieve 5kHz cutoff instead of the 6kHz, the following equation was used:

$$f = \frac{1}{2\pi\sqrt{C_8 C_9 R_8 R_9}}$$

where R8 and R9 values were chosen to be 3.3kOhms and determining C8, C9 to be 0.1uF capacitors (10000pF). Using a Sallen-Key filter generates an additional pole at the desired cut-

off frequency compared to a normal RC low-pass filter. This provides an additional -20dB/dec attenuation for high frequency signal(s), which often distorts the overall measured signal at the input. The overall gain of this stage was set to 2, defined by a non-inverting amplifier circuit where the following equation was used:

$$Av_1 = 1 + \frac{R_{10}}{R_{11}}$$

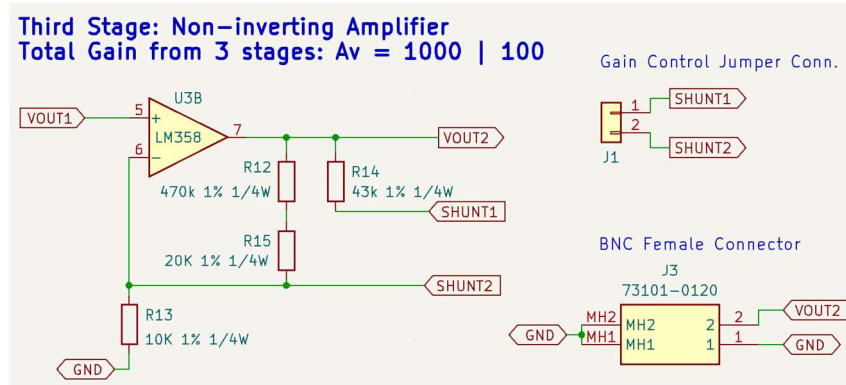


Figure 7) Third Stage Adjustable Gain Stage (Rev_01)

The third and last stage was designed to be the adjustable gain stage, which also implements the non-inverting amplifier circuit set by the following:

$$Av_2 = 1 + \frac{(R_{12} + R_{15})}{R_{13}}$$

The gain of this stage was set at 50, which is still within the frequency limit of the LM358 (with a gain of 50 and defined UGBW, the cutoff frequency of the op-amp is 24kHz.)

An overall gain of 1000 was achieved when amplified through all three stages. If the J1 connector is shorted together with a jumper, this introduces R14 in parallel with the feedback resistor network (R12 + R15); the reduced gain can be expressed in the following equation:

$$Av_{2_{Jumper\ Shorted}} = 1 + \frac{((R_{12} + R_{15}) \cdot R_{14})}{R_{13}(R_{14} + (R_{12} + R_{15}))}$$

With the jumper in place, the overall gain for the third stages reduces to 5, setting the overall gain of the amplifier to 100. A BNC connector was used as the output connector for the circuit as a normal receptacle for oscilloscopes or data-acquisition devices, to record and analyze the amplified measured signal.

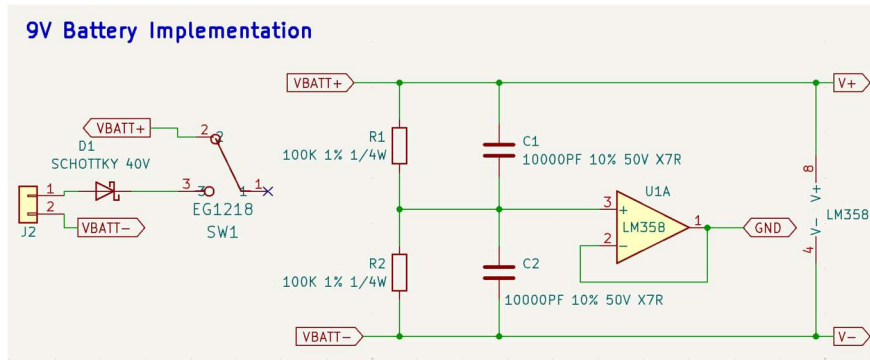


Figure 8) 9V Battery Circuit; Providing +4.5V and -4.5V Supply Rail (Rev_01)

To implement a 9V battery to power the device(s), acting as a +4.5V and -4.5V supply rail for the op-amps, the circuit above was added. To generate the dual supply rails, a resistive divider of R1 and R2 of equal values was added and connected to the buffer circuit U1A. The op-amp acts as a virtual ground for the supply rails, with the capacitive divider added in parallel to the resistors acting as additional decouple capacitors for the 2 rails. For additional protection, a Schottky diode and switch circuit was added to the input connection of the 9V battery. The Schottky diode acts as a protection element in case the polarities of the battery connection were reversed, and the switch was implemented to act as isolation element, allowing everything to be hooked up to the device and ensuring proper connection before providing power.

Initial Circuit Testing and Verification

All elements were populated onto the breadboard as seen in Figure X) and then tested using a function generator, an oscilloscope in the classroom laboratory and both a 9V battery and DC-power supply. A 1V peak-to-peak sinewave was provided from the function generator and attenuated through the resistor divider for a 1mV differential input, with a frequency set between 1.5Hz and 5kHz.

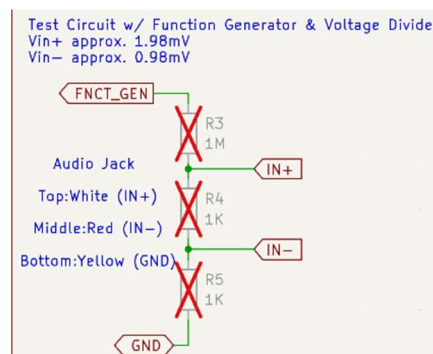


Figure 9) Neural Signal Emulation Test Circuit (move to initial testing section)

Both input and output signals were measured and compared with expected output peak-to-peak amplitude to be at least greater than 0.707 times the input, as this would represent a -3dB drop-off at the set cutoff frequencies. As the passive components used for this setup were not low tolerance rated, there is expected variation for the total gain of the circuit and where the cutoff frequencies are seen. This further extended the range of acceptable performance for this test-board circuit, of 20% variation allowed. The oscilloscope was able to measure 5kHz from both input and output channel. However, for the low-frequency cut-off (around less than 2-3Hz), the oscilloscope was unable to capture the frequency and provide said-value from the function generator. Therefore, the frequency value taken into consideration was 2Hz instead of 1.5Hz. To calculate the attenuation seen at the cutoff frequencies, the following equation was used:

$$A_v(dB) = 20 \log_{10} \left(\frac{V_{out_{pk_pk}}}{V_{in_{pk_pk}}} \right)$$

For the low frequency cutoff at 2Hz, the measured attenuation was approximately (0.78), resulting in -2.165dB roll-off and falls within the acceptable range. For the high-frequency cutoff at 5kHz, the measured attenuation was approximately (0.833), resulting in -1.584dB roll-off and right at the border for the acceptable range. Again, this was to be expected as the filter network consisted of 4 passive elements, therefore more susceptible to variations but this can be improved upon proper components with low tolerance are implemented.

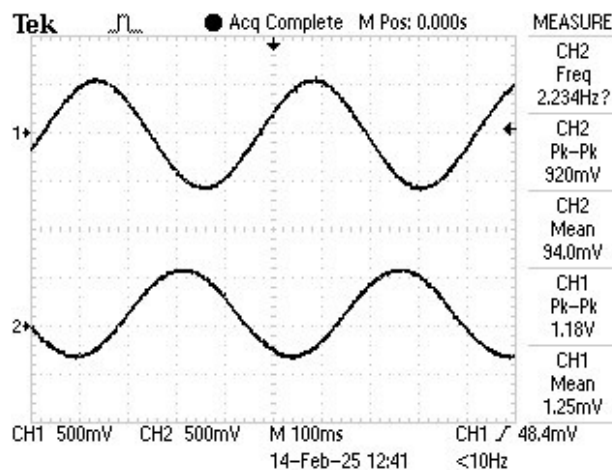


Figure 10) Input (Channel 1) vs Output (Channel 2) Signal Measured at ~ 1.5Hz

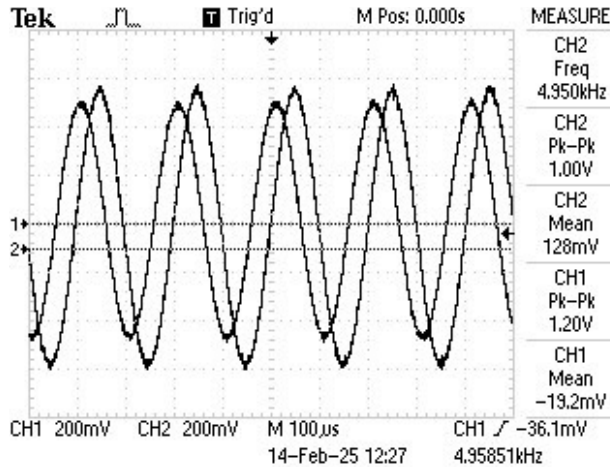


Figure 11) Input (Channel 1) vs Output (Channel 2) Signal Measured at ~5kHz

PCB Layout and Assembly

After validating the functionality of the breadboard circuit, using resistive voltage divider network to replicate input neural signals, the next step was to design the layout for the PCB. The project and PCB-layout were initialized in KiCAD, an open-source software EDA program, which can generate the necessary files to fabricate. To start, the complete circuit schematic was designed to define the associated footprints and associated nets for the PCB.

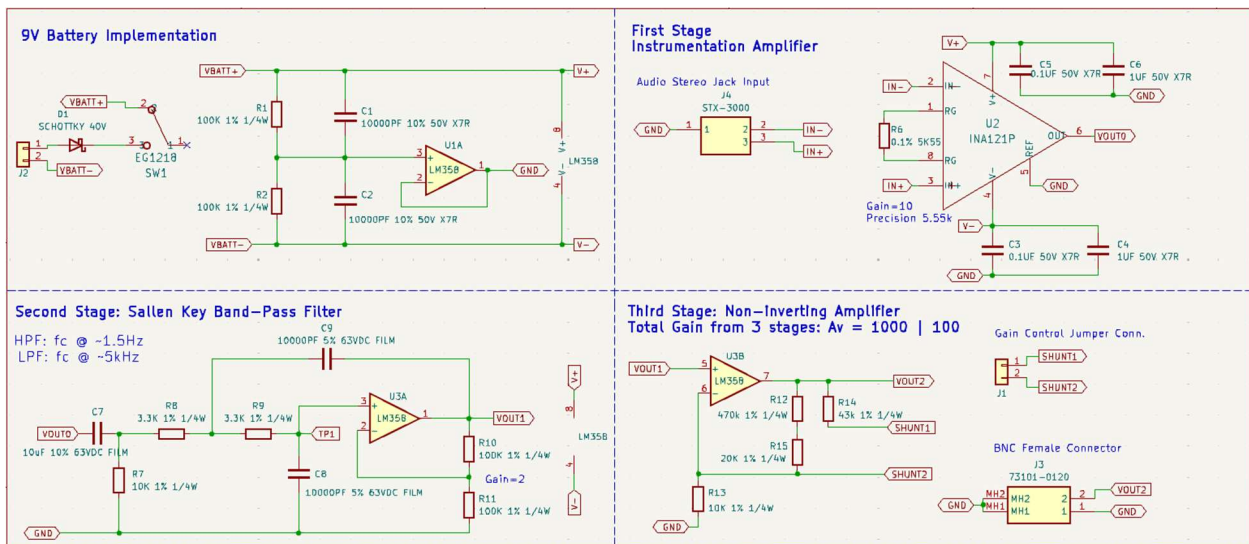


Figure 12) Circuit Schematic for Extracellular Voltage Amplifier (Rev_01) in KiCAD

The layout for the PCB was designed with the following considerations as signal integrity needs to be properly maintained, for operating in the low-frequency analog region. Since the input signal magnitude is expected to be within the μV region, the signal is highly subjected to noise

and external parasitic(s). Additionally, since the receptacles are going to be accessed externally using a stereo jack for the input, BNC connector for the output and jumpers for the 9V-battery, connector placement needs to be easily accessible while also considering compactness of the device (area minimized as much as possible).

The device was implemented using a 2-layer PCB, with the bottom layer dedicated to a continuous ground plane (GND-pour). This ground pour provides a low impedance return path for signal currents, which is crucial for minimizing voltage drops in the path and ensuring signal integrity. Using only discrete ground traces can result in higher-impedance paths leading to signal attenuation and potential issues with ground loops. Since the device only uses through-hole components, the bottom-layer ground plane provides a convenient and direct connection to the GND net for all relevant components.

The top-layer was primarily reserved for signal-traces and supply rail, while the bottom layer was used only to simplify routing in densely populated areas. For the differential input signal from the stereo jack (J4), the routing was carefully designed to be symmetrical and as short as possible when connecting to the first-stage instrumentation amplifier (U2). This was essential because the electrode input signals are highly sensitive to variations and can impact the quality of common-mode rejection provided by the instrumentation app. Beyond the instrumentation amplifier, all signal traces were routed to avoid overlapping or interleaving between layers, and signal directionality was kept consistent to minimize parasitic coupling and incorporating any additional noise into the recorded neural signal. Additional connectors were added throughout the circuit to incorporate testing-point connections at the output of each stage, to provide accessible ways of debugging the circuit. The complete PCB-layout area was measured to have a length and width of 92.4mm x 72.21mm and a comprised height of 19.56mm, set by the sizing of the components. Afterwards, the manufacturability of the layout was checked through KiCAD's design-rule-checker (DRC). [8] This feature indicates any sort of design violation that could prevent the fabrication-house from properly producing the PCB. KiCAD's DRC also encompassed the feature of verifying layout versus schematic design parity to ensure all the associated net connections in the layout matched the schematic net connections. Once there were no more errors indicated by DRC, the design files were comprised into fabrication outputs

consisting of Gerber (.gbr) and Drill (.drl) files that are necessary for PCB fabrication and required by the manufacturer. [8]

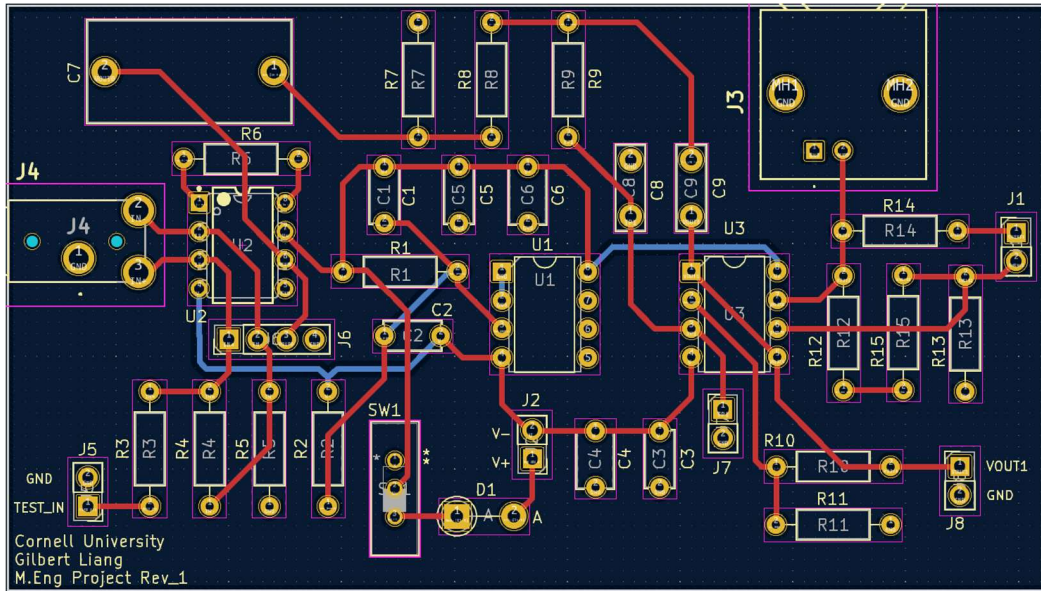


Figure 13) PCB Layout Extracellular Voltage Amplifier (Rev_01) in KiCAD

The PCB was fabricated through JLCPCB, a commonly used prototype fabrication manufacturer, and after a brief inspection, soldered and assembled in the testing laboratory. To verify all the connections and components were soldered properly, a handheld digital multimeter was used to conduct a continuity test. After completing the continuity test, the next step was to repeat the breadboard circuit test with the PCBA. To further emulate the testing conditions with the neural signal input, the resistive divider was soldered onto the ends of the stereo-jack connector, with the sinewave function generator connected in similar fashion as the test-circuit.



Figure 14) Soldered PCB Assembly (Rev_01)

During testing, an issue was observed regarding the power source used to operate the PCB. While the breadboard version of the circuit functioned the same with both a 9V battery and a 9V DC power supply, the PCB assembly exhibited abnormal behavior when powered by the DC supply. Specifically, the output signal either flat-lined near 0V or, in some cases, displayed a saturated 60 Hz AC waveform on the oscilloscope. This issue did not occur when the PCB was powered by a 9V battery, where the circuit performed as expected. Despite multiple verification steps, the root cause of this discrepancy could not be determined. However, since the intended use case for the final design involves battery-powered operation, further investigation into the power supply problem was deferred. Extensive testing was done with the PCB where the frequency of operation was swept across from 0.01Hz to 100kHz.

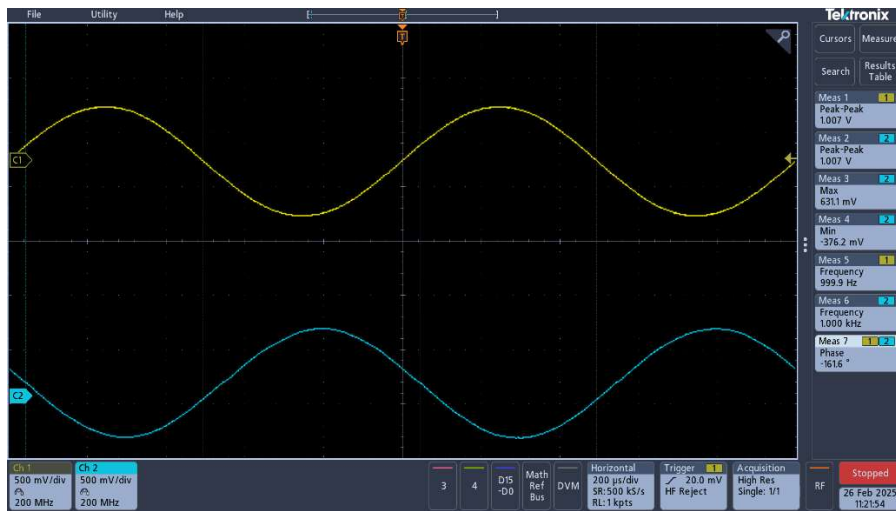


Figure 15) In-band Frequency Operation at 1kHz (Channel 1-Input | Channel 2-Output)

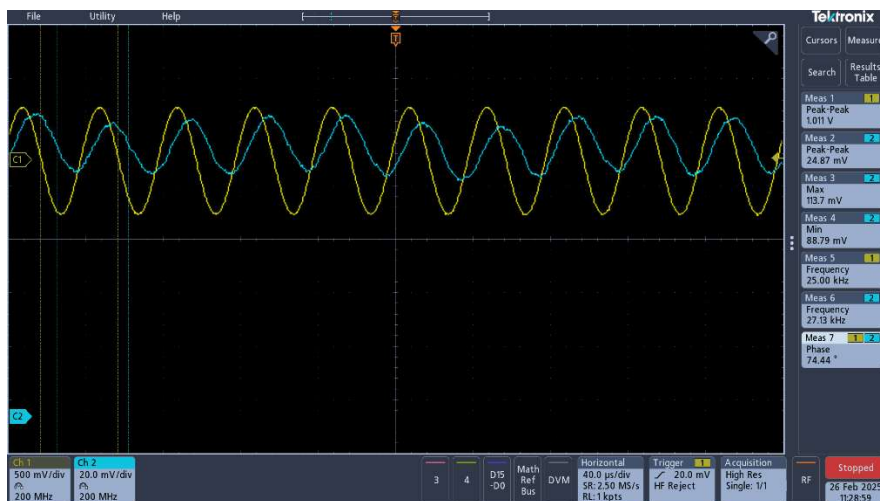


Figure 16) Frequency Operation at 25kHz (Channel 1-Input | Channel 2-Output)

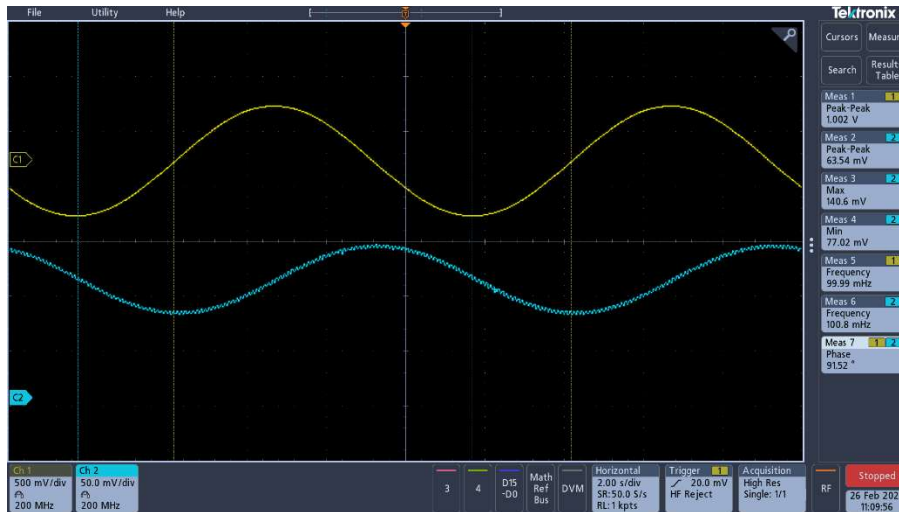


Figure 17) Frequency Operation at 100mHz (Channel 1-Input | Channel 2-Output)

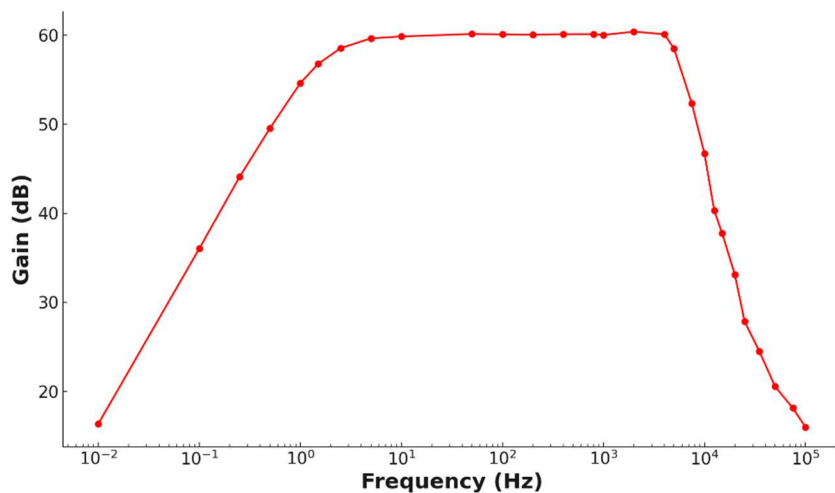


Figure 18) Magnitude Bode-Plot of PCB with gain of 1000

For the frequency plots shown above, an in-band frequency was used to verify the appropriate gain being applied (gain of 1000 = 60dB), where the measured output peak-to-peak voltage was very similar to the input voltage before attenuated by 1000. As for the out of band frequencies of the band-pass filter, both upper and lower limits were tested. For the upper limits, the output attenuation is expected to be -40dB/dec from the cutoff frequency of 5kHz. Given the measured output value at 25kHz was approximately 27db, a -32dB drop from the in-band frequencies, this would indicate the 2-pole filter taking into effect at the 5kHz cutoff frequency. Additionally, for the lower cutoff frequency, there's an expected zero at 0Hz which increases until the pole at that lower cutoff frequency takes into effect at 1.5Hz, neutralizing the zero and flattening the gain curve as seen above. To verify the +20dB/dec effect of the zero, the gain was measured at around

100mHz, slightly below a single decade from 1.5Hz, however the overall gain measured was approximately 36dB (-24dB from the desired cutoff), verifying the pole cancellation of the zero at 0Hz.

The power consumption of the PCB was measured by inserting an ammeter in series with the 9V battery at the supply rail. During operation, the measured current draw was approximately 1.8 mA, corresponding to 16.2mW of power. Given the circuit consists of three LM358 op-amp channels and an INA121P instrumentation amplifier, this value is consistent with the combined quiescent current specifications of the devices and additional power consumption from the passive resistive elements used for the gain-stages.

Crawdad Lab Experiment

Once the PCB and overall circuit functionality were verified to operate as intended, the board was brought to the ECE 4910 laboratory for live testing using the “Crawdad” experiment. In this lab, the commercial A-M Systems Model 1700 Differential AC Amplifier is used to amplify and filter extracellular signals recorded from a dissected crawfish tail. [3] The experiment involves immersing the dissected tail in a saline bath and applying electrical stimulation to produce action potential(s) along one of (or multiple) the six motor axons. A glass suction electrode is attached to the nerve, serving as the signal pickup and connecting to the positive terminal of the amplifier’s differential input. The saline bath, which encompasses the tissue, acts as the common ground and is connected to the negative terminal of the differential amplifier. The signal from the suction electrode is routed through a pin-jack connector, which interfaces with the PCB with the stereo-jack input.

While this configuration introduces some signal attenuation, since the connection from nerve to amplifier is not direct, it still presents a very low impedance path and is sufficient for capturing the evoked extracellular action potentials. As for the output of the voltage amplifier, the amplified and filtered signal is sent to a data-acquisition device that allows the data to be processed and read through the laboratory computer. The program being used to display the recorded data from the DAQ is LabChart v8.1.

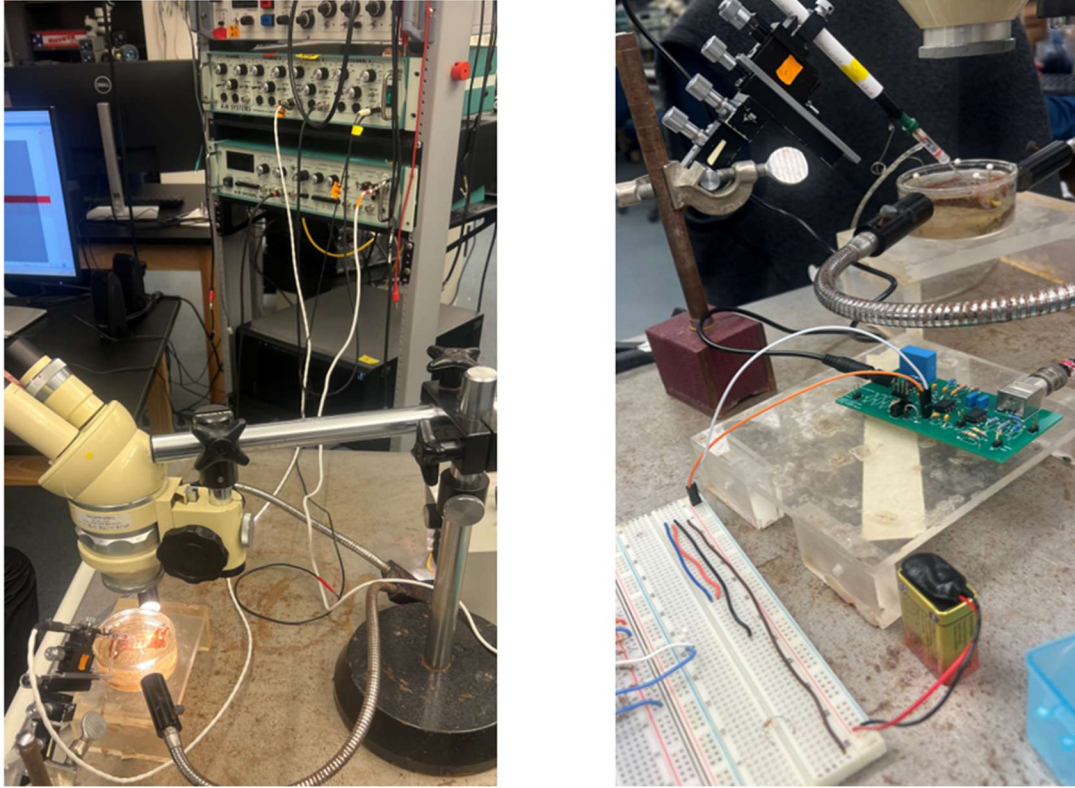


Figure 19) i) Crawdad Setup using A-M 1700 amp. ii) Crawdad Setup using designed PCB

Both devices were used to measure the motor nerve activity produced by the stimulated crawfish tail. Some of the factors that had to be considered when comparing the recorded data between one another: 1) Temperature of the crawfish tail can affect the quality of the action potential as they are normally stored in cold temperatures before tested on and begin to warm up, the longer it is left out. [3] 2) Connectivity of the suction-electrode for the extracted nerve can also vary as this process is done by hand in the experiment. When using suction electrodes, the recorded voltage amplitude can vary significantly depending on how well the electrode is coupled to the nerve. Factors such as the tightness of the seal between the glass electrode and the nerve, the electrode tip diameter relative to the nerve size, and the consistency of saline contact all affect the quality of the electrical interface. [2] A weaker or less stable seal can result in poorer signal coupling, increased impedance, thus lower recorded amplitudes and/or increased noise. However, a tight, stable seal maximizes signal transfer and minimizes common-mode noise, improving the overall signal-to-noise ratio (SNR).

In the context of analyzing extracellular action potentials, the most relevant information lies in the timing and frequency of spike occurrences, rather than their absolute voltage amplitudes.

While recorded amplitudes may vary due to factors such as electrode placement, seal quality, and tissue variability, the shape and temporal pattern of the spikes remain consistent and physiologically meaningful. Therefore, if the signal-to-noise ratio is sufficient to detect action potential from background noise, meaningful analysis can be performed based on the latency, inter-spike intervals, and firing frequency of the neural responses. As for the recorded lab experiment, the commercial A-M 1700 amplifier was initially used to measure the action potential of the crawfish tail followed by the designed PCB voltage amplifier.

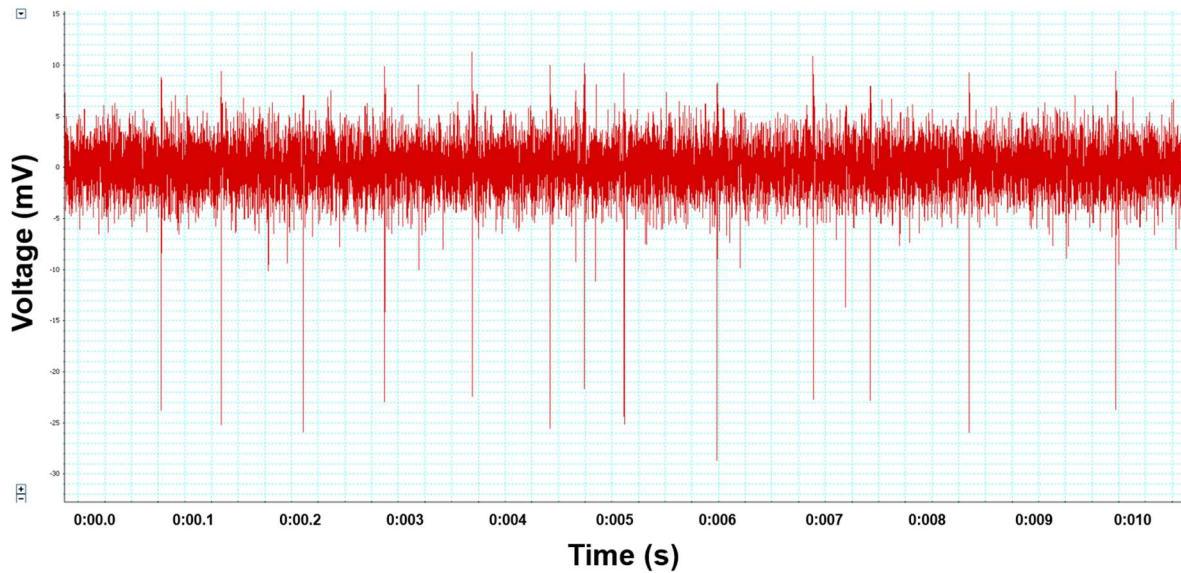


Figure 20) A-M 1700 Action Potential Crawdad Motor Nerve Recording (0.01s snapshot)

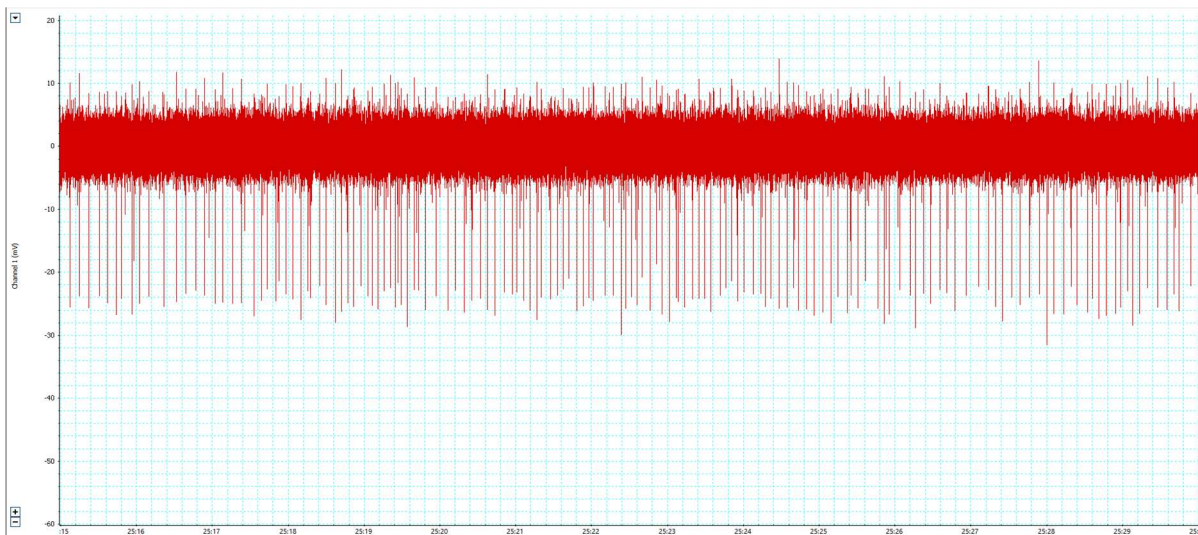


Figure 21) A-M 1700 Action Potential Crawdad Motor Nerve Recording (15s snapshot)

A 15 second snapshot was taken from the recording of the measured motor nerve as well as a 0.01 second snapshot to further analyze the amplitude of the action potential and the noise floor.

The commercial amplifier was set to a gain of 1000, with a lower cutoff frequency of 300Hz and a higher cutoff frequency of 5kHz as this is the preferred bandwidth for measuring motor nerve action potential signals. For measuring other types of neural signals, the range of the bandpass frequency will vary. The overall noise floor for the commercial amplifier was measured from -5mV to 5mV, (10mV peak to peak) with action potential signals ranging from -25mV to 10mV (35mV peak to peak). The calculated SNR from taking the measurements of the noise floor and action potential amplitudes is approximately 3.5:1.

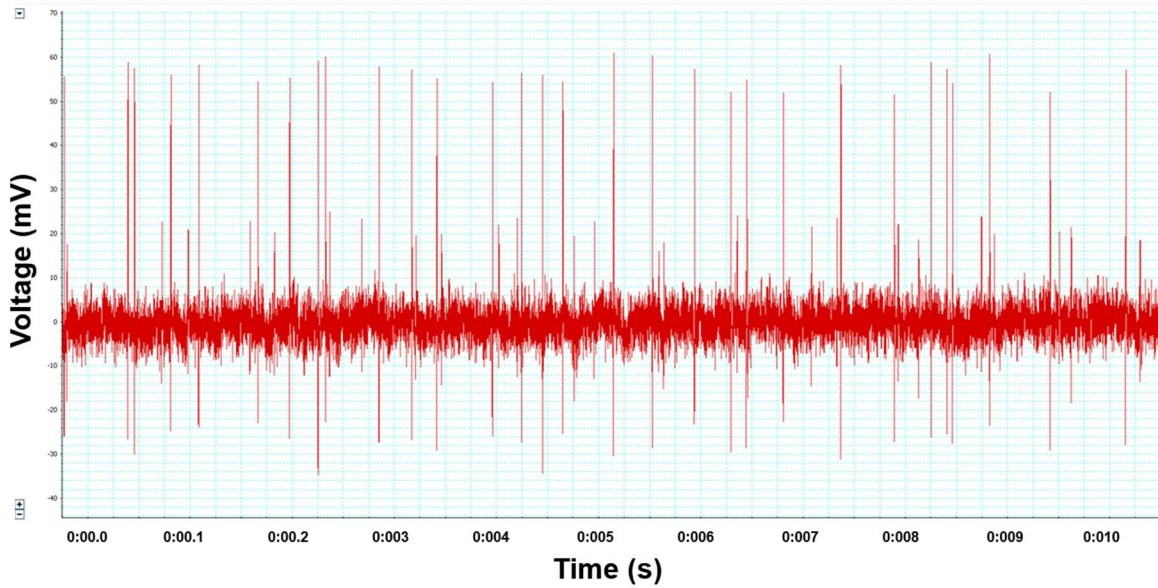


Figure 22) PCB Action Potential Crawdad Motor Nerve Recording (0.01s snapshot)

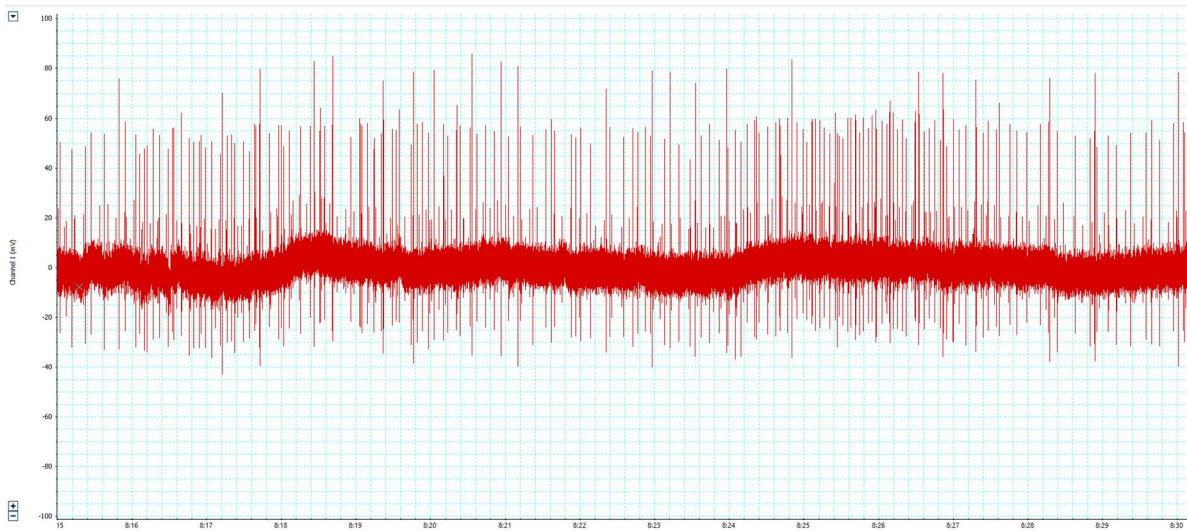


Figure 23) PCB Action Potential Crawdad Motor Nerve Recording (15s snapshot)

For the PCB-recorded signal, both the noise floor and action potential amplitude were measured to be approximately double those of the commercial amplifier. Specifically, the PCB's noise floor ranged from -10 mV to $+10$ mV (20 mV peak-to-peak), while the recorded action potentials ranged from -25 mV to $+60$ mV (85 mV peak-to-peak). When calculating the signal-to-noise ratio (SNR) using the same method applied to the commercial A-M 1700 amplifier, the PCB achieved an approximate SNR of 4.5:1, indicating that both systems provide comparable SNR performance.

However, the PCB amplifier exhibited a less stable noise floor, with noticeable baseline drift compared to the commercial amplifier. This behavior is primarily attributed to the low-frequency cutoff of the PCB amplifier being set at 1.5 Hz, which is significantly lower than the 300 Hz cutoff of the commercial system. As a result, the PCB failed to adequately attenuate low-frequency interference, including environmental noise and physiological drift. The most prominent source of interference likely coupled into the device is 60 Hz AC power-line noise, which can modulate the baseline and contribute to the observed instability. Increasing the high-pass cutoff frequency to 300 Hz would better suppress these low-frequency components and improve baseline stability in future iterations.

Conclusion & Next Steps

This project successfully demonstrated the design, fabrication, and validation of a low-cost voltage amplifier for extracellular neural signal recording. The amplifier was tested in a live biological setting during the Crawdad lab experiment, where action potentials were recorded from the dissected motor nerve of a crawfish tail. The performance of the custom-designed PCB amplifier was directly compared to the commercial voltage amplifier, A-M Systems Model 1700 Differential AC Amplifier.

The amplifier achieved an in-band gain of approximately 60 dB (gain of 1000) and reliably captured action potential signals with a measured (SNR) of approximately 4.5:1, comparable to the commercial system. Frequency-domain testing confirmed expected behavior from the band-pass filter design, including -40 dB/dec attenuation above the 5kHz cutoff and $+20$ dB/dec gain slope below the 1.5 Hz lower cutoff.

Despite comparable SNR, the PCB amplifier had a less stable noise floor than the A-M 1700, mainly due to the low high-pass cutoff frequency of 1.5 Hz. This allowed unwanted low-frequency noise and baseline drift, including coupling of 60 Hz AC interference. Nonetheless, the overall design proved successful in capturing clean neural signals using a significantly simplified and low-cost solution.

A key achievement of this work was the substantial cost reduction. The commercial A-M 1700 amplifier costs approximately \$782.50 per channel, whereas the custom amplifier developed in this M.Eng project costs only ~\$32 per channel in materials. This represents a ~96% cost reduction, making the system highly cost efficient for educational labs and resource-constrained research environments.

As for the next steps, this consists of several opportunities, to further enhance the functionality, stability, and scalability of the amplifier device:

- Design a metal enclosure for the PCB to reduce ambient electromagnetic interference (EMI). Even though the test table was grounded, interference was still observed during recordings. A dedicated metal enclosure would act as a local Faraday cage, improving noise rejection.
- Increase the high-pass cutoff frequency to 300 Hz to attenuate low-frequency drift and power-line interference, stabilizing the baseline during long recordings.
- Add adjustable filtering functionality, allowing users to tune the low and high cutoff frequencies to accommodate different experimental bandwidths.
- Redesign gain distribution across the three amplification stages to minimize input-referred noise and enhance dynamic range.
- Integrate multiple amplifier channels on a single PCB to support multi-channel or parallel recordings, further improving cost efficiency.

References:

- [1] B. Land, "ECE 5030 Biomedical Electronics Lecture Notes," School of Electrical and Computer Engineering, Cornell University, Ithaca, NY, USA. Available: <https://people.ece.cornell.edu/land/courses/ece5030/>
- [2] B. R. Land, R. A. Wytttenbach, and B. R. Johnson, "Tools for physiology labs: an inexpensive high-performance amplifier and electrode for extracellular recording," *Journal of Neuroscience Methods*, vol. 106, no. 1, pp. 47–55, 2001. Available: [https://doi.org/10.1016/S0165-0270\(01\)00328-4](https://doi.org/10.1016/S0165-0270(01)00328-4)
- [3] B. R. Johnson, "Crawdad Lab 2: Motor nerve recording," *Emory University Crawdad Lab Manual*, [Online]. Available: <https://faculty.college.emory.edu/sites/wytttenbach/crawdad/2.NerveRecording.html>.
- [4] A-M Systems, "Model 1700 Differential AC Amplifier," *Biomedical Instruments Trading*, [Online]. Available: <https://www.biomedical-instruments-trading.com/products/electrophysiology/amplifiers/differential-extracellular/84-a-m-systems-model-1700>.
- [5] LOW COST EXTRACELLULAR VOLTAGE AMPLIFIER, Cornell University [Online] https://vanhunteradams.com/6930/Pawan_Perera.pdf
- [6] Texas Instruments, *INA121: FET-Input, Low Power Instrumentation Amplifier*, Datasheet, May 1998. [Online]. Available: <https://www.ti.com/lit/ds/symlink/ina121.pdf>
- [7] Texas Instruments, *LM358: Dual Operational Amplifier*, Datasheet, Rev. J, October 2015. [Online]. Available: <https://www.ti.com/lit/ds/symlink/lm358.pdf>
- [8] KiCAD, "KiCAD EDA, Version 8.0," Mar. 2024. [Online]. Available: <https://www.kicad.org/>.

Appendix

Item Number	RefDes	Part Description	Manufacturer	MFPN	DPN	PPU	Qty	Cost
1	U1, U3	IC OPAMP GP 2 CIRCUIT 8DIP	Texas Instruments	LM358AP	296-9554-5-ND	\$0.27	2	\$0.54
2	U2	IC INST AMP 1 CIRCUIT 8DIP	Texas Instruments	INA121P	INA121P-ND	\$9.47	1	\$9.47
3	C1, C2	CAP CER 10000PF 10% 50V X7R RADIAL	Kemet	C315C103K5R5TA	399-4148-ND	\$0.23	2	\$0.46
4	C8, C9	CAP FILM 10000PF 5% 63VDC RADIAL	EPCOS - TDK Electronics	B32529C0103J000	495-1097-ND	\$0.25	2	\$0.50
5	C3, C5	CAP CER 0.1UF 50V X7R RADIAL	Vishay Beyschlag/Draloric/BC Components	K104K10X7RF5UH5	BC2665CT-ND	\$0.25	2	\$0.50
6	C4, C6	CAP CER 1UF 50V X7R AXIAL (needs to be changed to electrolytic)	KEMET	C420C105K5R5TA91707200	399-C420C105K5R5TA91707200 CT-ND	\$0.41	2	\$0.82
7	C7	CAP FILM 10UF 10% 63VDC RADIAL	EPCOS - TDK Electronics	B32522C0106K000	495-4092-ND	\$2.50	1	\$2.50
8	R1, R2,	RES 100K OHM 1% 1/4W AXIAL	YAGEO	MFR-25FRF52-100K	13-MFR-25FRF52-100KCT-ND	\$0.10	4	\$0.40
11	R6	Metal Film Resistors - Through Hole MFB/SMA 0207-25 0.1% CECC 06 C1 5K55	Vishay Beyschlag/Draloric/BC Components	MBB0207VD5551BC100	594-MBB0207VD5551BC1	\$1.24	1	\$1.24
12	R7, R13	RES 10K OHM 1% 1/4W AXIAL	YAGEO	MFR-25FRF52-10K	13-MFR-25FRF52-10KCT-ND	\$0.10	2	\$0.20
13	R8, R9	RES 3.3K OHM 1% 1/4W AXIAL	YAGEO	MFR-25FBF52-3K3	MFR-25FBF52-3K3-ND	\$0.10	2	\$0.20
14	R12	RES 470K OHM 1% 1/4W AXIAL	KOA Speer Electronics, Inc.	MF1/4DCT52R4703F	2019-MF1/4DCT52R4703FCT-ND	\$0.15	1	\$0.15
15	R15	RES 20K OHM 1% 1/4W AXIAL	KOA Speer Electronics, Inc.	MF1/4DCT52R2002F	2019-MF1/4DCT52R2002FCT-ND	\$0.15	1	\$0.15
16	R14	RES 43K OHM 1% 1/4W AXIAL	YAGEO	MFR-25FBF52-43K	MFR-25FBF52-43K-ND	\$0.10	1	\$0.10
17	D1	SCHOTTKY DO15 40V 1A 150C	STMicroelectronics	1N5819	497-6610-1-ND	\$0.22	1	\$0.22
18	J1, J2, J5, J7, J8	CONN HEADER VERT 2POS 2.54MM	Würth Elektronik	61300211121	732-5315-ND	\$0.12	5	\$0.60
19	J3	CONN BNC RCPT R/A 75 OHM PCB	Molex	731010120	WM5508-ND	\$1.74	1	\$1.74
20	J4	CONN JACK STEREO 3.5MM TH R/A	Kycon, Inc.	STX-3000	2092-STX-3000-ND	\$0.71	1	\$0.71
21	SW1	SWITCH SLIDE SPDT 200MA 30V	E-Switch	EG1218	EG1903-ND	\$0.80	1	\$0.80
	External eBOM							
	Misc.	BATTERY ALKALINE 9V	Panasonic	6LF22XWA/B	P687-ND	\$2.32	1	\$2.32
	Misc.	JUMPER W/TEST PNT 1X2PINS 2.54MM	Würth Elektronik	60900213421	732-2678-ND	\$0.28	1	\$0.28
	Misc.	JLC-PCB (5-PCB + Shipping)	JLCPCB	-	-	\$21.66	1	\$4.33
		JLC-PCB (5-PCB + Shipping + Assembly)				\$32.00	-	-
		BOM Cost if self-assembling						\$28.23

Figure 24) Bill of Materials (Including PCB Fabrication Costs) for Device